Materials Science and Engineering C 75 (2017) 425–432

Contents lists available at ScienceDirect

Materials Science and Engineering C

journal homepage: www.elsevier.com/locate/msec

Modeling of drug release behavior of pH and temperature sensitive poly(NIPAAm-*co*-AAc) IPN hydrogels using response surface methodology and artificial neural networks

Sanogo Brahima, Cihangir Boztepe, Asim Kunkul, Mehmet Yuceer *

Faculty of Engineering, Department of Chemical Engineering, Inonu University, Malatya, Turkey

ARTICLE INFO

Article history:
Received 14 November 2016
Received in revised form 21 December 2016
Accepted 15 February 2017
Available online 20 February 2017

Keywords:
Smart hydrogel
IPN
Drug release
RSM
ANN

ABSTRACT

An interpenetrated polymer network (IPN) poly(NIPAAm-*co*-AAc) hydrogel was synthesized by two polymerization method: emulsion and solution polymerization. The pH- and temperature-sensitive hydrogel was loaded by swelling with riboflavin drug, a B2 vitamin. The release of riboflavin as a function of time has been achieved under different pH and temperature environments. The determination of experimental conditions and the analysis of drug delivery results were achieved using response surface methodology (RSM). In this work, artificial neural networks (ANNs) in MATLAB were also used to model the release data. The predictions from the ANN model, which associated input variables, produced results showing good agreement with experimental data compared to the RSM results.

1. Introduction

The study of hydrogels has gained great potential in recent years because of their properties and high capacity to absorb large quantities of water. Hydrogels play an important role in many fields, such as tissue engineering scaffolds, biosensors, BioMEMS devices, and drug carriers [1,2]. Among these applications, hydrogel-based drug delivery systems have become a major area of research interest and many products have been developed [3,4]. Their unique properties make them useful for delivering biomolecules. One of the important characteristics of hydrogels is their responsiveness to stimuli, which can be easily tailored into hydrogel networks during fabrication [5,6]. The mechanical properties of hydrogels and their swelling and shrinking behaviors change in response to physical or chemical stimuli, such as temperature, pH, ionic strength, solvent composition and electric fields. These characteristics make hydrogels intelligent materials and thus potential devices for drug delivery [7,8]. Hydrogels that are sensitive to temperature and pH are the most frequently used because they exploit changes in temperature and pH as triggering agents for controlled release of drugs [9,10]. One of the most popular thermosensitive polymers is poly(*N*-isopropylacrylamide) because it possesses a phase transition temperature (lower critical solution temperature, LCST) in water close to human body temperature (32 °C), making it very attractive for biomedical applications [11–13]. The cross-linked hydrogel swells below the LCST and collapses above the LCST, which is a desirable behavior used for pulsed release of drugs [14,15]. According to the targeted applications, to obtain a much more favorable system that is sensitive to several stimuli simultaneously, *N*-isopropylacrylamide (NIPAAm) is copolymerized with ionic monomers [16]. To prepare pH and temperature responsive hydrogels, the combination of acrylic acid (AAc), an anionic monomer, and NIPAAm is mainly used because AAc is hydrophilic and can increase the volume phase transition temperature (VPTT) [17,18].

The loading of hydrophilic drug molecules such as riboflavin to hydrogel matrix from aqueous solution by hydrogel swelling is relatively simple method. The loading of drug molecules into stimuli-responsive hydrogel matrix is depended on hydrogel swelling behavior. On the other hand, release of drug from the hydrogels is depended on deswelling behavior [19]. The hydrogel swelling capacity increases with increasing AAc content because of electrostatic repulsion between the polymer chains. Poly(NIPAAm-*co*-AAc) hydrogels with 10% AAc (molar ratio) contents have a broad phase transition at near the human body temperature [20,21].

The synthesis of hydrogels is accomplished through different types of methods, one of which is an interpenetrated polymer network (IPN). This type of hydrogel consists of two or more interpenetrating polymer networks made in one or two steps [22]. In the two step IPN type, the hydrogel synthesized in the first step is dried and then re-swelled in a solution containing the monomers and a suitable cross-linking agent that will react to give the IPN

* Corresponding author.
E-mail address: mehmet.yuceer@inonu.edu.tr (M. Yuceer).

http://dx.doi.org/10.1016/j.msec.2017.02.081
0928-4931/

Table 1
Independent variables in central composite design and their levels for drug release investigations.

Independent variables	Symbol	Lower limit	Upper limit
pH (X_1)	A	2.00	12.00
Temperature (°C) (X_2)	B	22.00	52.00
Time (min) (X_3)	C	3.00	420.00

structure hydrogel [23,24]. The synthesis of hydrogels through the IPN method allows the improvement of the elastic and mechanical properties of the resulting gel compared to those synthesized by other methods [25,26].

The accuracy of mathematical modeling can also play an important role in the success of drug delivery devices, such as in the design of intelligent networks. Moreover, mathematical modeling presents some advantages, such as limiting the number of experiments and contributing to enhanced performance [27].

Response surface methodology (RSM), which is a combination of mathematical and statistical methods, is useful for data analysis and modeling in different fields of engineering. Additionally, RSM allows the determination of optimum operating conditions of the system, as shown by the response surfaces influenced by several process variables, and computation of the relationship between input parameters and developed response surfaces [28,29].

Artificial neural networks are powerful tools that are built under the basis of the functioning of the human neuron system, which computes the relationship between input and output data [30,31]. They can be successfully used to model difficult and complex problems [32,33]. Boztepe et al. found good results by using ANNs to model the swelling behaviors of acrylamide-based hydrogels [34].

In this study, using the thermosensitive NIPA monomer and pH sensitive AAc as a comonomer, poly(NIPA-*co*-AAc) microgels were synthesized by free radical emulsion polymerization. Then, poly(NIPAAm-*co*-AAc) interpenetrated network (IPN) hydrogels were prepared by free radical solution polymerization in the presence of pre-synthesized poly(NIPAAm-*co*-AAc) microgels. The synthesized IPN poly(NIPAAm-*co*-AAc) hydrogel was loaded with riboflavin (B2 vitamin) and the drug releases were performed in different mediums under various pH and temperature conditions. Drug release modeling was performed using response surface methodology (RSM)-central composite design of Design Expert-10 software (trial-version) and artificial neural networks (ANNs) in MATLAB.

Table 2
The proposed experimental design.

Experience no	pH	Temperature (°C)	Time (min)	% release
1	7.00	52.00	3.00	6.28
2	7.00	37.00	211.50	59.3
3	7.00	37.00	211.50	59.3
4	12.00	37.00	420.00	42.1
5	12.00	22.00	211.50	37.5
6	2.00	37.00	420.00	62.4
7	2.00	37.00	3.00	11.1
8	7.00	37.00	211.50	59.2
9	7.00	22.00	420.00	43.6
10	2.00	22.00	211.50	49.6
11	7.00	37.00	211.50	59.26
12	2.00	52.00	211.50	75
13	12.00	52.00	211.50	45.1
14	7.00	22.00	3.00	3.3
15	7.00	37.00	211.50	59.3
16	7.00	52.00	420.00	91.5
17	12.00	37.00	3.00	4.2

Table 3
Percentage of drug released amount.

Temperature(°C)	pH 2	pH 3	pH 4	pH 5	pH 7	pH 11	pH 12
22	50.54	48.43	48.05	40.04	43.6	37.22	37.46
30	57.38	53.54	51.10	42.52	44.07	38.35	40.37
37	62.45	54.66	53.87	50.60	69.57	39.72	42.05
40	62.77	61.20	58.79	54.71	70.89	41.94	42.94
45	77.97	77.02	71.92	54.43	76.52	49.70	52.98
52	76	61.56	60.48	56.31	91.47	44.07	45.10

2. Materials and methods

2.1. Materials

N-isopropylacrylamide as a monomer (NIPAAm, from Merck, Germany) was crystallized from ethanol solution under reduced pressure at 30 °C. Acrylic acid (AAc, from Sigma-Aldrich, Germany) was used as a monomer, *N*,*N*′-methylenebisacrylamide (MBAAm, from Merck, Germany) was used as the crosslinker, and sodium dodecyl sulfate was used as the surfactant (SDS, from Sigma-Aldrich, Germany). Ammonium persulfate (APS, from Merck, Germany) and tetraethylenemethylenediamine (TEMED, from Merck, Germany) were used as an initiator and an accelerator, respectively. Because the chemicals were of high purity, they were used without further purification.

2.2. Synthesis of poly(NIPAAm-co-AAc) microgels by emulsion polymerization

The synthesis of poly(NIPAAm-*co*-AAc) microgels was performed in a three-necked flask. The microgels were prepared by free radical polymerization. In 150 ml of distilled water heated at 80 °C under stirring at 750 rpm, 0.15 g (0.52 mmol) of sodium dodecyl sulfate dissolved in 30 ml of water was added. Then, 2.8 g (24.74 mmol) of *N*-isopropylacrylamide (NIPAAm) monomer, 2.5 ml (2.47 mmol) of acrylic acid (AAc) as a comonomer and 0.08 g (0.519 mmol) of *N*,*N*-methylene-bis-acrylamide (MBA) as a crosslinker dissolved in 10 ml of water was added. A small amount of EDTA was added to the flask as a stabilizer. The reaction mixture was purged with pure nitrogen gas for 20 min to remove excess oxygen. After 30 min, 0.15 g of initiator APS dissolved in 10 ml of water was added drop wise to the mixture to begin the polymerization reaction. After 3 h, the temperature and stirring speed were adjusted to 52 °C and 750 rpm, respectively, and the emulsion polymerization continued for 24 h. To remove the unreacted monomers, surfactant and initiator, the obtained microgels were dialyzed in a membrane for one week while periodically changing the water.

2.3. Synthesis of IPN poly(NIPAAm-co-AAc) hydrogel by solution polymerization

To synthesize an interpenetrated polymer network (IPN) hydrogel, the poly(NIPAAm-*co*-AAc) microgels formed by emulsion polymerization were used in the solution polymerization. First, 0.1 g of poly(NIPAAm-*co*-AAc) microgels, 0.25 g (2.209 mmol) of NIPAAm

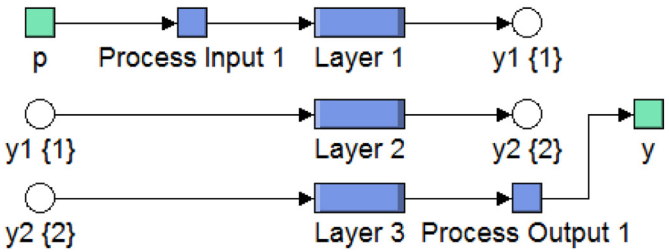

Fig. 1. Three layers of neural network block diagram.

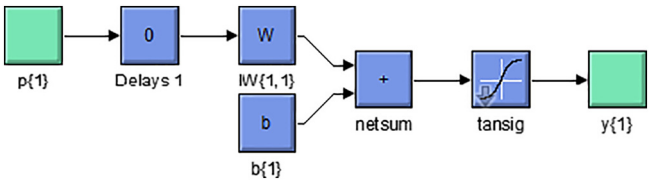

Fig. 2. Input layer simulation.

monomer, 0.22 ml (0.22 mmol) of acrylic acid solution as a comonomer and 7.5 mg of MBA as a crosslinker were placed in a glass tube (6 mm diameter) and the mixture was left for 24 h in an ice bath. The reaction mixture was purged by pure nitrogen gas for 20 min to remove excess oxygen. Then, 0.25 ml of TEMED (1 g = 100 ml) and 0.20 ml of APS (5 g = 100 ml) were added to the hydrogel solutions. The hydrogels, obtained in soft, elastic long cylindrical shapes, were cut into 20-mm-long pieces. To remove the unreacted reagents, the hydrogels were left for one week in distilled water, which was renewed daily. The samples were dried in air and then under a vacuum at 40 °C until they reached a constant mass.

2.4. Swelling measurements

To determine the equilibrium swelling capacity and swelling kinetics of the synthesized IPN poly(NIPAAm-*co*-AAc) hydrogel, the dried hydrogel was placed in distilled water at pH 7 at laboratory temperature. At defined time intervals, the sample was removed from the water and weighed until the mass reached equilibrium.

The swelling ratio (S) of the hydrogel was calculated from Eq. (1)

$$S = \frac{m_t - m_0}{m_0} \tag{1}$$

where m_t and m_0 are the masses of the swollen hydrogels at time t and dry hydrogels, respectively [35].

2.5. Riboflavin loading into IPN poly(NIPAAm-co-AAc) hydrogel matrix

A synthesized dry IPN poly(NIPAAm-*co*-AAc) hydrogel disc was immersed in 50 ml of 200 ppm riboflavin solution. In this manner, riboflavin molecules penetrate the hydrogel's matrix by the swelling of the gel over 2 days. The loaded drug amount was determined by calculating the difference between the amount of riboflavin in solution before and after drug loading. The amount of drug was calculated using a standard curve of riboflavin drawn from samples analyzed on a UV-spectrophotometer at 445 nm, which is defined as the maximum absorbance of riboflavin. The amount of maximum drug loaded (average of 3 hydrogel discs) was 21.33 mg/g.

2.6. Riboflavin release from IPN poly(NIPAAm-co-AAc) hydrogel matrix

After drying the surface with paper, the loaded hydrogels were transferred to 50 ml of aqueous solution at defined pH and temperature conditions. All of the release experiments were performed in a temperature range of 22–52 °C and a pH range of 2–12. The amount of drug released in the medium was determined by UV-spectrophotometry, in

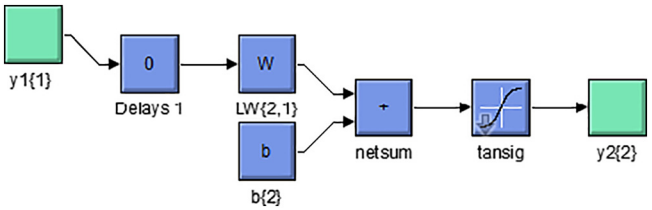

Fig. 3. Hidden layer simulation.

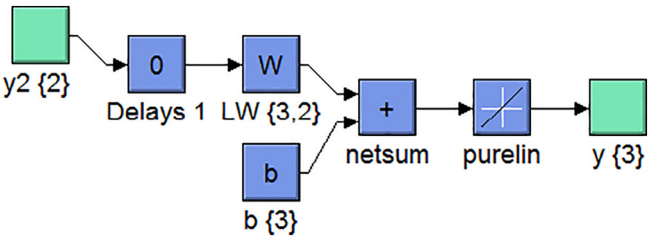

Fig. 4. Output layer simulation.

which 0.5 ml of the solution containing the drug was periodically removed for UV analysis at 445 nm and by using a standard calibration curve for riboflavin. The 0.5 ml of solution removed for each analysis was replaced by the same amount of fresh solution. The percentages of drug released were calculated by taking into account the amounts loaded using the following equation [36]:

$$\text{Released riboflavin amount} = \frac{M_t}{M_{Rb}} \times 100 \tag{2}$$

where M_t is the amount of riboflavin released at time t and M_{Rb} is the amount of riboflavin loaded into the hydrogel.

2.7. Experimental design

Experimental design was conducted by Design Expert-10 (trial) software. Independent variables were defined and at different ranges were introduced to the software, which has created models. As a result, a quadratic (2nd degree) model was suggested and the accuracy of the proposed model was tested by analysis of variance (ANOVA). For the optimization of drug release from hydrogel, the independent variables in the design of experiments and their limit values are shown in Table 1.

In Table 2, by using variable limit values for the experimental design, 17 experiments were proposed and executed, after which the responses were determined. Independent variables and their response values are shown in Table 3.

For development of the model, the results were correlated using a response function (Eq. (3)).

$$\begin{aligned} Y &= \beta_0 + \beta_1 X_1 + \beta_2 X_2 + \beta_{12} X_1 X_2 + \beta_{11} X_1^2 + \beta_{22} X_2^2 + \ldots \\ Y &= \beta_0 + \sum_{i=1}^{k} \beta_i X_i + \sum_{i<j}^{k} \beta_{ij} X_i X_j + \sum_{i=1}^{k} \beta_{ii} X_i^2 + \ldots \end{aligned} \tag{3}$$

where Y is the response of % drug released, X represents the design variables (pH, temperature and time) and β represents the model coefficients (determine by the least squares method).

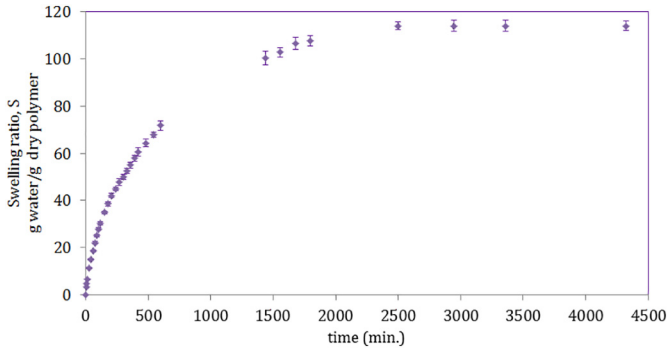

Fig. 5. IPN poly (NIPAAm-*co*-AAc) hydrogel swelling graphic. Results are reported as mean ± standard deviation of the mean ($n = 3$).

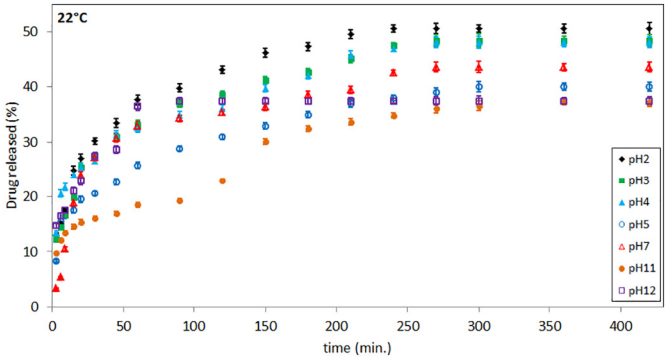

Fig. 6. Release of riboflavin as a function of time at 22 °C in various pH for the hydrogels samples loaded with same initial amounts of drug. Results are reported as mean ± standard deviation of the mean ($n = 3$).

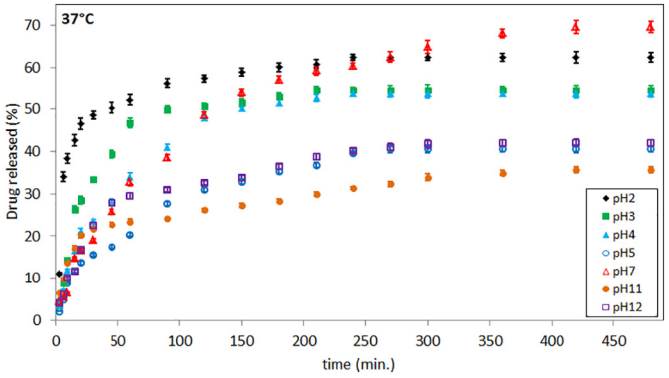

Fig. 8. Release of riboflavin as a function of time at 37 °C in various pH for the hydrogels samples loaded with same initial amounts of drug. Results are reported as mean ± standard deviation of the mean ($n = 3$).

2.8. Artificial neural networks design

For the estimation of the drug release amount, three layer feed-forward back propagation networks were used. The number of neurons was defined as 3 in the input layer, 30 in the hidden (or central) layer and 1 in the output layer of the network. A tangential sigmoid transfer function was used between the first two layers, and a linear function was used between the hidden and output layers. The number of hidden layers and the number of neurons in the layers were determined by trial-and-error.

The developed artificial neural network is exported to Simulink environment using the '*gensim*' command after the training is finished. Fig. 1 shows the ANN block diagram in MATLAB-Simulink environment. The block diagram of neural network model for input layer is shown in Fig. 2. Block diagrams of the neural network model for hidden layer and output layer are shown in Figs. 3 and 4, respectively.

The transfer functions tangent sigmoid used in this study are given in Eq. (4).

$$y_i = \frac{2}{1 + e^{-2\,z_i}} - 1 \tag{4}$$

where z_i is the input of the neuron in hidden layer and y_i is the output of neuron while calculating $z_i x_i$, tansig transfer function was calculated a layer's output from its net input.

IW, LW and b are defined as input weight, layer weight and bias, respectively. The ANN model is summarized in the following Eqs. (5)–(7);

$$y_1 = \text{tansig}[\text{IW}\{1,1\}\cdot p + b_1] \tag{5}$$

$$y_2 = \text{tansig}[\text{LW}\{2,1\}\cdot y_1 + b_2] \tag{6}$$

$$y_3 = \text{purelin}[\text{LW}\{3,2\}\cdot y_2 + b_3] \tag{7}$$

where y_i are ith output of layers. ANN model output is defined as y_3.

The Levenberg-Marquardt optimization method was used for network training and for weight adjusting. In the experimental studies, a total of 784 data points were obtained, which were normalized prior to being introduced to the network. In total, 70% of the data (549 data point) were randomly picked for training the network, and the remaining 235 data points were used to test the model. The ANN model inputs consist of three variables: time (min), pH and temperature (°C). For the development of ANN model, the neural network toolbox in MATLAB was used. With the help of written code, the data sets were introduced to the network in MATLAB. After training was performed and the most appropriate network architecture was executed, the network structure was recorded and the model was created. The success of the developed model was measured by statistical techniques.

3. Results and discussion

3.1. Hydrogel swelling results

The figure below shows the swelling kinetics of the synthesized IPN poly(NIPA-*co*-AAc) hydrogel.

As shown in Fig. 5, the dried hydrogel swells when placed in distilled water. The swelling of the hydrogel is attributed to the presence of hydrophilic amide (NH_2) and carboxylic (COOH) groups in the structures of the NIPA and AAc monomers, respectively, which are the groups in the hydrogel structure that absorb water. The maximum degree of swelling obtained in the hydrogel was 114 (equilibrium state).

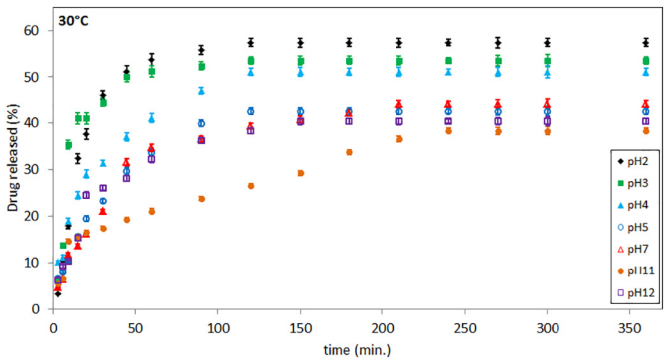

Fig. 7. Release of riboflavin as a function of time at 30 °C in various pH for the hydrogels samples loaded with same initial amounts of drug. Results are reported as mean ± standard deviation of the mean ($n = 3$).

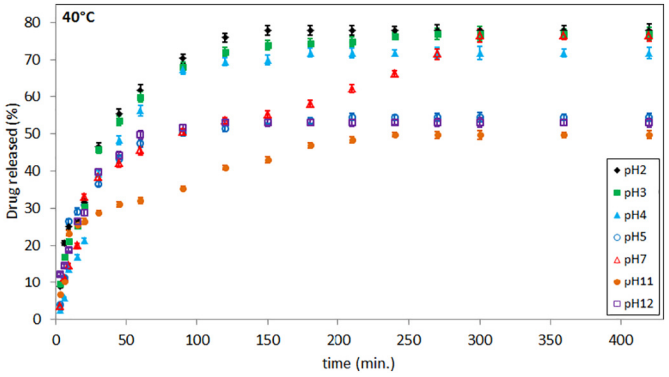

Fig. 9. Release of riboflavin as a function of time at 40 °C in various pH for the hydrogels samples loaded with same initial amounts of drug. Results are reported as mean ± standard deviation of the mean ($n = 3$).

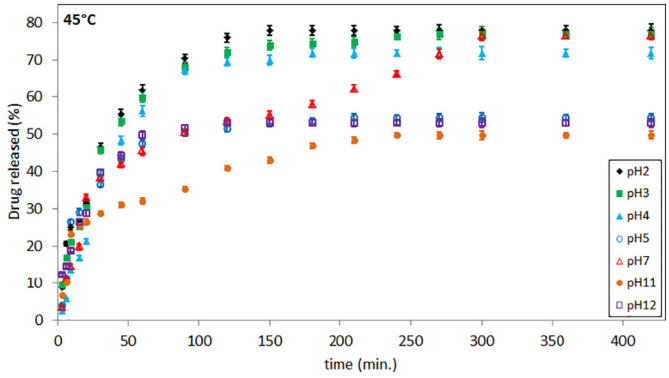

Fig. 10. Release of riboflavin as a function of time at 45 °C in various pH for the hydrogels samples loaded with same initial amounts of drug. Results are reported as mean ± standard deviation of the mean ($n = 3$).

3.2. Results of riboflavin release

The graphics below show the riboflavin release profiles in different mediums under various temperature and pH conditions (Figs. 6–11).

The riboflavin release profiles of IPN poly(NIPAAm-*co*-AAC) hydrogel loaded with 21.33 mg/g polymer at various temperatures and pH levels were investigated. The amount of drug released was observed to increase along with temperature, which is attributed to the presence of hydrophobic groups in the backbone of the hydrogel. When the temperature increased to the critical temperature of NIPAAm, the hydrogel shrinks and the drug is released into the medium. The drug release amount also increases when the medium acidity increases because of the presence of anionic groups (COOH) in the hydrogel structure, which cause shrinking of the hydrogel. This shrinking of the hydrogel as a result of pH leads to diffusion of the drug out of the hydrogel's matrix. This result can also explain the low release degree observed in the basic mediums compared to the acidic mediums.

The release rate is much more rapid when the temperature is increased and when the pH is more acidic. A large amount of drug is released initially but then the release rate decreases.

In this series of releases, the largest amounts of riboflavin released were observed at a temperature of 52 °C at pH 7 (91.47%), followed by 45 °C at pH 2 (77.97%). This result shows the key roles (major) played by temperature and pH in the drug delivery system from the poly(NIPA-*co*-AAc) hydrogel matrix. The abrupt decrease of the hydrogel as a result of these two factors also appears to influence the polymer structure, which impact drug release by imprisoning some drug molecules. This situation was the case for the release at 52 °C at pH 2, pH 3, pH 4, pH 11 and pH 12, where the release amounts were less than

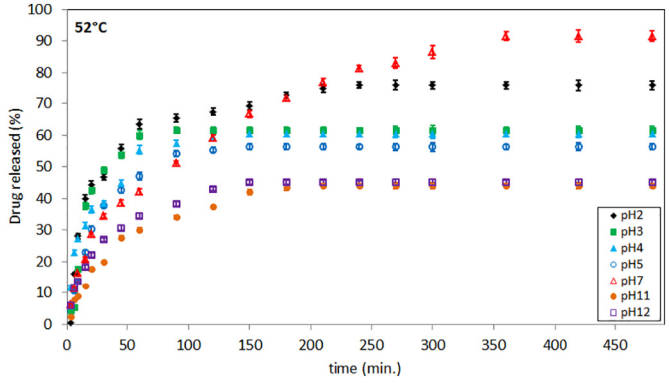

Fig. 11. Release of riboflavin as a function of time at 52 °C in various pH for the hydrogels samples loaded with same initial amounts of drug. Results are reported as mean ± standard deviation of the mean ($n = 3$).

Table 4
ANOVA results.

Source	Sum of squares	F value	Prob > F	
Model	1.03	34.42	<0.0001	Important
A	0.060	18.05	0.0038	
B	0.088	26.48	0.0013	
C	0.58	173.42	<0.0001	
A2	0.020	5.95	0.0448	
B2	1.617×10^{-4}	0.049	0.8317	
C2	0.21	64.07	<0.0001	
AB	7.921×10^{-3}	2.38	0.1664	
AC	4.523×10^{-3}	1.36	0.2815	
BC	0.050	15.19	0.0059	
Residual	0.023			

that at 45 °C for the same pH values. During all of the experiments, not all of the drug molecules were released. This occurrence can be attributed to the collapse of the hydrogel chains and volume shrinkage of the gel, which limits the release of all drug molecules because some drugs become entrapped in the shrunken matrix. As previously shown in the literature, drug molecules released out of hydrogel matrix systems can sometimes be complex. The release first begins with the diffusion of drug molecules close to the outer surface, followed by diffusion of drug molecules at a slightly farther distance. Drug molecules at the center can experience difficulty reaching the outer surface, which explains why the entire drug load could not be released in the experiments.

3.3. RSM results

For the hydrogel release amount optimization, the ANOVA model test results are presented in Table 4.

The equations for the amount of drug released from the hydrogel are shown below (Eqs. (8) and (9)) in coded and real factor terms, respectively.

$$\text{Release amount} = 0.59 - 0.087 \cdot A + 0.10 \cdot B + 0.27 \cdot C - 0.069 \cdot A^2 - 6.198 \cdot 10^{-3} \cdot B^2 - 0.22 \cdot C^2 - 0.044 \cdot A \cdot B - 0.034 \cdot A \cdot C + 0.11 \cdot B \cdot C \quad (8)$$

$$\text{Release amount} = -0.14071 + 0.049835 \cdot pH + 5.58723 \cdot 10^{-3} \cdot T + 2.37180 \cdot 10^{-3} \cdot t - 2.74090 \cdot 10^{-3} \cdot pH^2 - 2.75444 \cdot 10^{-5} \cdot T^2 - 5.17163 \cdot 10^{-6} \cdot t^2 - 5.93333 \cdot 10^{-4} \cdot pH \cdot T - 3.22542 \cdot 10^{-5} \cdot pH \cdot t + 3.59073 \cdot 10^{-5} \cdot T \cdot t \quad (9)$$

T: temperature; t: time.

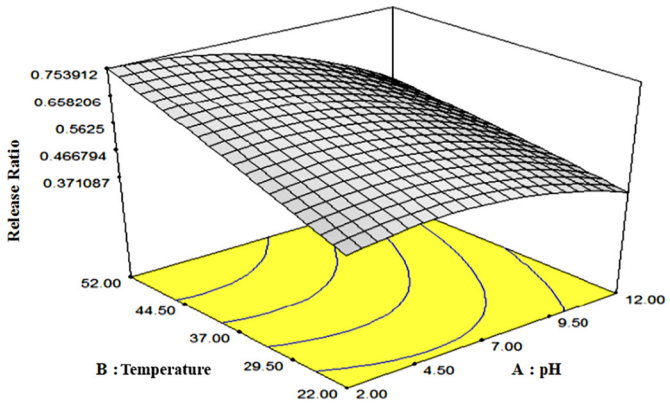

Fig. 12. Effect of pH and temperature factors on the release amount.

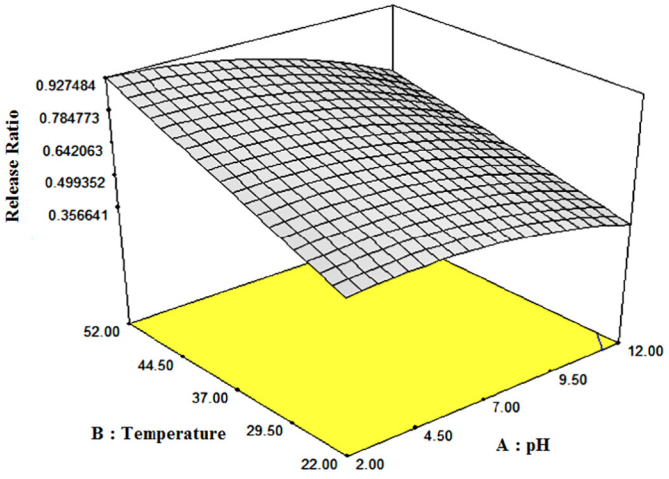

Fig. 13. Optimization results that maximized the release amount.

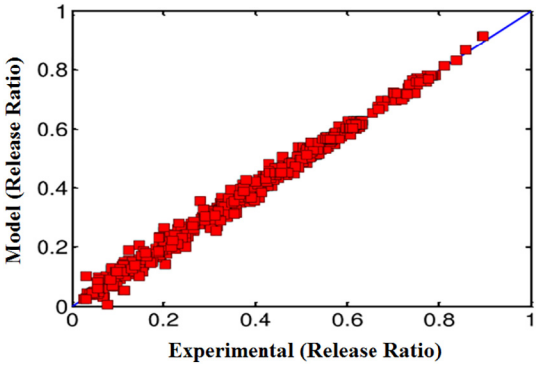

Fig. 14. ANN training results.

At 211.5 min, the effects of pH and temperature on the release rate are shown by the 3D graphic in Fig. 12. The maximized release rate from the optimization results is shown in Fig. 13. According to the results, at pH = 2.42, temperature = 51.58 °C and time = 345.82 min, the release rate is predicted to be approximately 0.92.

3.4. ANN modeling results

The data obtained in the experimental studies were modeled by ANNs and the success of the developed model was tested by statistical

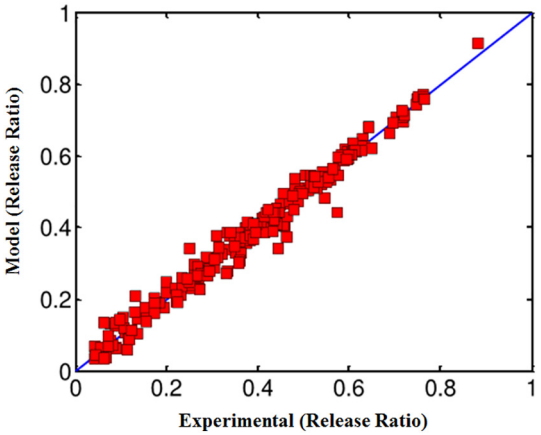

Fig. 15. ANN test results.

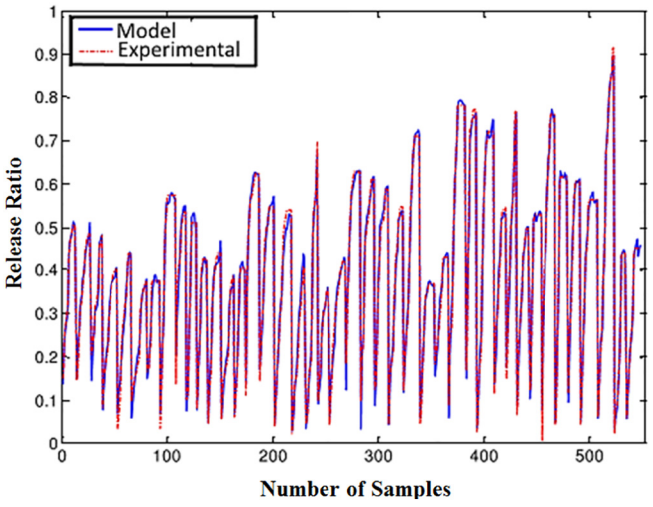

Fig. 16. For ANN training data experimental-model fit.

methods. Comparisons of the ANN model and experimental data for the training and testing data are shown in Figs. 14 and 15, respectively. Additionally, comparison of experimental data and the model predictions is presented in another form in Figs. 16 and 17.

To evaluate the success of the model, four statistical evaluation functions were calculated and presented in Table 5: Root Mean Square Error (RMSE), Mean Square Error (MSE), Mean Absolute Percentage Error (MAPE) (%) and Correlation Coefficient (R). The equations for the statistical evaluation functions used in this study are given below (Eqs. (10)–(13)).

$$R = \frac{\sum_{i=1}^{N}(X_i-\overline{X})(Y_i-\overline{Y})}{\sqrt{\sum_{i=1}^{N}(X_i-\overline{X})^2}\sqrt{\sum_{i=1}^{N}(Y_i-\overline{Y})^2}} \tag{10}$$

$$RMSE = \sqrt{\frac{\sum_{i=1}^{N}(Y_i-Y_i)^2}{N}} \tag{11}$$

$$MAPE\ (\%) = \frac{1}{N}\sum_{i=1}^{N}\left(\left|\frac{Y_i-X_i}{X_i}\right|\right)\cdot 100 \tag{12}$$

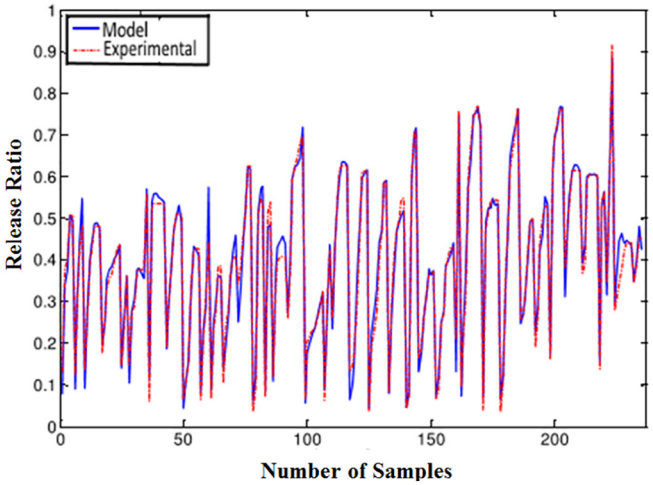

Fig. 17. For ANN test data experimental-model fit.

Table 5
Evaluation of ANN model results.

Training data					Test data			
Model	R	MAPE (%)	RMSE	MSE	R	MAPE (%)	RMSE	MSE
ANN	0.9953	6.4348	0.0188	3.5405×10^{-4}	0.9894	8.3087	0.0274	7.5081×10^{-4}

Table 6
Evaluation of RSM model results.

All data				
Model	R	MAPE (%)	RMSE	MSE
RSM	0.8439	119.3	0.1334	0.0179

$$MSE = \frac{1}{N}\sum_{i=1}^{N}(Y_i - X_i)^2 \quad (13)$$

where,

X_i: i. experimental value,

Y_i: i. predicted value,

N: number of data points,

$\overline{X}$: mean of experimental data,

$\overline{Y}$: mean of the values obtained from the model.

As observed in the tables and graphics above, the ANNs developed a successful model that can be used properly to examine the drug release from IPN poly(NIPA-*co*-AAc) hydrogels.

In this study, by examining Tables 5 and 6, the comparison of models developed by ANNs and RSM clearly shows that the ANN model is more efficient than the model developed by RSM. Because the experiments were conducted in a certain number and region, the RSM method was unable to predict the rise and fall of the previous values to produce models based on RSM design data. This result is attributed to the fact that the proposed RSM model was quadratic. However, with more data obtained under additional conditions, the mentioned rise and fall between values was evaluated by modeling of the experimental data by ANN, the results of which led to the development of a model. The RSM model and graphical representation of the experimental data are shown in Fig. 18.

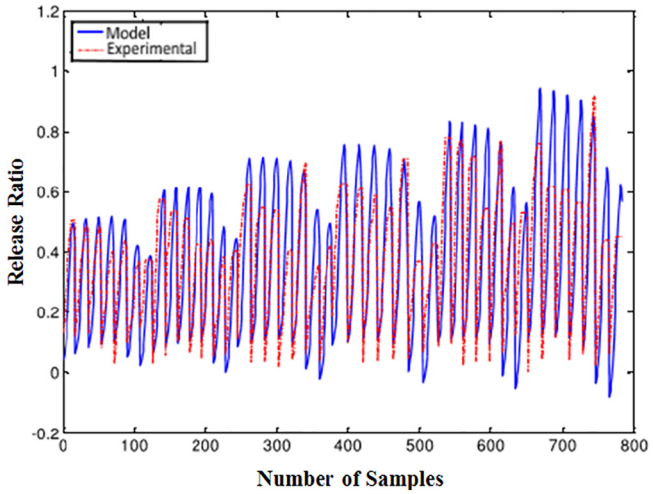

Fig. 18. Experimental-RSM model fit.

4. Conclusion

The drug delivery results from the IPN poly(NIPAAm-*co*-AAc) hydrogel show that pH and temperature play key roles in drug release. Generally, the drug release amount increased with increasing temperature as well as increasing acidity of the medium. In each series of experimentation, the maximum riboflavin release amount was achieved at the highest temperatures of 52 °C at pH 7 (91.47%) and 45 °C at pH 2 (77.97%). The drug delivery experimental results were used to develop models with RSM and ANNs. The evaluation of the two models using statistical evaluation functions (R, MAPE, RMSE and MSE) showed that the ANN model produced better results than the RSM model. The experimental results obtained were successfully modeled with artificial neural network methodology has great advantage of generality over the drug release behavior of hydrogels. The developed ANN model can thus be used efficiently to predict drug release behavior from hydrogels.

Acknowledgements

This work was supported by the Inonu University Research Fund [project number: İ.Ü.B.A.P. 2015-22].

References

[1] F. Ullah, M.B.H. Othman, F. Javed, Z. Ahmad, H.A. Akil, Classification, processing and application of hydrogels: a review, Mater. Sci. Eng. C 57 (2015) 414–433.
[2] A. Bashari, N.H. Nejad, A. Pourjavadi, Applications of stimuli responsive hydrogels: a textile engineering approach, J. Text. Inst. 11 (2013) 1145–1155.
[3] M.A. Haq, Y. Su, D. Wang, Mechanical properties of PNIPAM based hydrogels: a review, Mater. Sci. Eng. C 70 (2017) 842–855.
[4] H. Weng, J. Zhou, L. Tang, Z. Hu, Tissue responses to thermally-responsive hydrogel nanoparticles, J. Biomater. Sci. Polym. Ed. 9 (2004) 1167–1180.
[5] Y. Qiu, K. Park, Environment-sensitive hydrogels for drug delivery, Adv. Drug Deliv. Rev. 53 (2001) 321–339.
[6] J. Chen, K. Park, Superporous hydrogels: fast responsive hydrogel systems, Pure Appl. Chem. 36 (1999) 917–930.
[7] J. Chen, M. Liu, H. Liu, L. Ma, Synthesis, swelling and drug release behavior of poly(*N*,*N*-diethylacrylamide-*co*-*N*-hydroxymethyl acrylamide) hydrogel, Mater. Sci. Eng. C 29 (2009) 2116–2123.
[8] M.B. El-Arnaouty, M. Eid, M.A. Ghaffar, Radiation synthesis of stimuli responsive micro-porous hydrogels for controlled drug release of aspirin, Polym.-Plast. Technol. Eng. 54 (2015) 1215–1222.
[9] G. Fundueanu, M. Constantin, F. Bortolotti, P. Ascenzi, R. Cortesi, E. Menegatti, Preparation and characterisation of thermoresponsive poly(*N*-isopropylacrylamide-*co*-acrylamide-co-hydroxyethyl acrylate) microspheres as a matrix for the pulsed release of drugs, Macromol. Biosci. 5 (2005) 955–964.
[10] A. Islam, T. Yasin, Controlled delivery of drug from pH sensitive chitosan/poly(vinyl alcohol) blend, Carbohydr. Polym. 88 (2012) 1055–1060.
[11] A.M. Atta, S.A. Ahmed, Chemically crosslinked pH- and temperature-sensitive (*N*-isopropylacrylamide-co-1-vinyl- 2-pyrrolidone) based on new crosslinker, J. Dispers. Sci. Technol. 31 (2010) 1552–1560.
[12] H.G. Schild, Poly (*N*-isopropylacrylamide): experiment, theory and application, Prog. Polym. Sci. 17 (1992) 163–249.
[13] G. Fu, W.O. Soboyejo, Swelling and diffusion characteristics of modified poly (*N*-isopropylacrylamide) hydrogels, Mater. Sci. Eng. C 30 (2010) 8–13.
[14] D.C. Coughlan, F.P. Quilty, O.I. Corrigan, Effect of drug physicochemical properties on swelling/deswelling kinetics and pulsatile drug release from thermoresponsive poly(*N*-sopropylacrylamide) hydrogels, J. Control. Release 98 (2004) 97–114.
[15] Q. Yan, A.S. Hoffman, Synthesis of macroporous hydrogels with rapid swelling and deswelling properties for delivery of macromolecules, Polymer 36 (1995) 887–889.
[16] H. Naeem, Z. Farooqi, L. Shah, M. Siddiq, Synthesis and characterization of p(NIPAM-AA-AAm) microgels for tuning of optical properties of silver nanoparticles, J. Polym. Res. 19 (2014) 1–10.
[17] Y. Yu, Y. Liu, Y. Kong, E. Zhang, F. Jia, S. Li, Synthesis and characterization of temperature-sensitive poly(*N*-isopropylacryamide) hydrogel with comonomer and semi-IPN material, Polym.-Plast. Technol. Eng. 51 (2012) 854–860.
[18] W.A. Laftah, S. Hashim, A.N. Ibrahim, Polymer hydrogels: a rewiew, Polym.-Plast. Technol. Eng. 50 (2011) 1475–1486.

[19] T.R. Hoare, D.S. Kohane, Hydrogels in drug delivery: progress and challenges, Polymer 49 (2008) 1993–2007.
[20] A. Burmistrova, M. Richter, M. Eisele, C. Uzum, R. von Klitzing, The effect of co-monomer content on the swelling/shrinking and mechanical behaviour of individually adsorbed PNIPAM microgel particles, Polymer 3 (2011) 1575–1590.
[21] I. Haider, M. Siddiq, S.M. Shah, S. Rehman, Synthesis and characterization of multi-responsive poly (NIPAm-*co*-AAc) microgels, Mater. Sci. Eng. 60 (2004) 1–10.
[22] A.K. Bajpai, S.K. Shukla, S. Bhanu, S. Kankane, Responsive polymers in controlled drug delivery, Prog. Polym. Sci. 33 (2008) 1088–1114.
[23] A.C. Wenceslau, F.G. Santos, É.R.F. Ramos, C.V. Nakamura, A.F. Rubira, E.C. Muniz, Thermo- and pH-sensitive IPN hydrogels based on PNIPAAm and PVA-Ma networks with LCST tailored close to human body temperature, Mater. Sci. Eng. 33 (2012) 1259–1265.
[24] M.R. Moura, F.A. Aouada, M.R. Guilherme, E. Radovanovic, A.F. Rubira, E.C. Muniz, Thermo-sensitive IPN hydrogels composed of PNIPAAm gels supported on alginate-Ca^{2+} with LCST tailored close to human body temperature, Polym. Test. 25 (2006) 961–969.
[25] M. Shivashankar, B.K. Mandal, A review on interpenetrating polymer network, Int. J. Pharm. Pharm. Sci. 4 (2012) 1–7.
[26] J. Wang, J. Li, One-pot synthesis of IPN hydrogels with enhanced mechanical strength for synergistic adsorption of basic dyes, Soft Mater. 13 (2015) 160–166.
[27] C.C. Lin, A.T. Metters, Hydrogels in controlled release formulations: network design and mathematical modeling, Adv. Drug Deliv. Rev. 58 (2006) 1379–1408.
[28] M. Nourani, M. Baghdadi, M. Javan, G.N. Bidhendi, Production of a biodegradable flocculant from cotton and evaluation of its performance in coagulation-flocculation of kaolin clay suspension: optimization through response surface methodology (RSM), J. Environ. Chem. Eng. 4 (2016) 1996–2003.
[29] F.A. Chaibva, R.B. Walker, The use of response surface methodology for the formulation and optimization of salbutamol sulfate hydrophilic matrix sustained release tablets, Pharm. Dev. Technol. 17 (2012) 594–606.
[30] M. Yuceer, Artificial neural network models for HFCS isomerization process, Neural Comput. & Applic. 19 (2010) 979–986.
[31] M. Yuceer, Z. Yildiz, T. Abbasov, Evaluation of electromagnetic filtration efficiency using LS-SVM, Physicochem. Probl. Miner. Process. 51 (2015) 73–187.
[32] A. Sarimeseli, M. Yuceer, Investigation of infrared drying behaviour of spinach leaves using ANN methodology and dried product quality, Chem. Process. Eng. 36 (4) (2015) 425–436.
[33] D. Imren, M.L. Koc, M. Gumusderelioglu, Prediction of the pH and the temperature-dependent swelling behavior of -alginate hydrogels by artificial neural networks, Int. J. Nat. Eng. Sci. 3 (2009) 127–132.
[34] C. Boztepe, M. Solener, M. Yuceer, A. Kunkul, O.S. Kabasakal, Modeling of swelling behaviors of acrylamide-based polymeric hydrogels by intelligent system, J. Dispers. Sci. Technol. 36 (2015) 1647–1656.
[35] B. Mandal, S.K. Ray, Swelling, diffusion, network parameters and adsorption properties of IPN hydrogel of chitosan and acrylic copolymer, Mater. Sci. Eng. C 44 (2014) 132–143.
[36] G.R. Mahdavinia, H. Etemadi, In situ synthesis of magnetic CaraPVA IPN nanocomposite hydrogels and controlled drug release, Mater. Sci. Eng. C 45 (2014) 250–260.